Broad antibiotic resistance profile of the subclass B3 metallo-beta-lactamase GOB-1, a di-zinc enzyme

the FEBS Journal

Broad antibiotic resistance profile of the subclass B3 metallo-β-lactamase GOB-1, a di-zinc enzyme

Louise E. Horsfall[1], Youssef Izougarhane[1], Patricia Lassaux[1], Nathalie Selevsek[2], Benoit M. R. Liénard[3], Laurent Poirel[4], Michael B. Kupper[5], Kurt M. Hoffmann[5], Jean-Marie Frère[1], Moreno Galleni[1] and Carine Bebrone[1]

1 Centre d'Ingénierie des Protéines, Université de Liège, Belgium
2 Department of Biochemical Engineering, Saarland University, Saarbrucken, Germany
3 Chemistry Research Laboratory, University of Oxford, UK
4 Service de Bactériologie-Virologie, INSERM U914 ''Emerging Resistance to Antibiotics'', Hôpital de Bicêtre, Assistance Publique/Hôpitaux de Paris, Faculté de Médecine Paris Sud, K.-Bicêtre, France
5 Institute of Molecular Biotechnology, RWTH-Aachen University, Germany

Keywords
antibiotic resistance; GOB; metallo-β-lactamase; zinc-binding site; β-lactamase

Correspondence
C. Bebrone, Centre d'Ingénierie des Protéines, Université de Liège, Allée de 6 Aout B6, Sart-Tilman, Liège, Belgium
Fax: +32 43 663 364
Tel: +32 43 663 348
E-mail: Carine.Bebrone@ulg.ac.be
Website: http://www.cip.ulg.ac.be

(Received 16 September 2010, revised 5 January 2011, accepted 4 February 2011)

doi:10.1111/j.1742-4658.2011.08046.x

The metallo-β-lactamase (MBL) GOB-1 was expressed via a T7 expression system in *Escherichia coli* BL21(DE3). The MBL was purified to homogeneity and shown to exhibit a broad substrate profile, hydrolyzing all the tested β-lactam compounds efficiently. The GOB enzymes are unique among MBLs due to the presence of a glutamine residue at position 116, a zinc-binding residue in all known class B1 and B3 MBL structures. Here we produced and studied the Q116A, Q116N and Q116H mutants. The substrate profiles were similar for each mutant, but with significantly reduced activity compared with that of the wild-type. In contrast to the Q116H enzyme, which bound two zinc ions just like the wild-type, only one zinc ion is present in Q116A and Q116N. These results suggest that the Q116 residue plays a role in the binding of the zinc ion in the QHH site.

Introduction

Metallo-β-lactamases (MBLs) belong to class B of the β-lactamases [1–3]. All MBLs exhibit the αβ/βα sandwich fold [4] and unlike the enzymes of other classes (A, C and D), which all contain a nucleophilic serine residue in their active site, the MBLs utilize zinc to perform hydrolysis [5,6]. The heterogeneous class of MBLs is further divided into three groups (B1, B2 and B3) according to substrate specificity and sequence similarity [7]. Subclass B2 has a narrow substrate spectrum limited to carbapenems [8], whereas subclasses B1 and B3 have broad substrate spectra, with B3 showing preferential activity for cephalosporins [9,10].

Subclass B1 contains IMP and VIM variants, as well as NDM-1, which are encoded by mobile genetic elements, posing the greatest threat of all the MBLs. Also present in the group are the well-characterized MBLs of *Bacillus cereus* (BcII), which was the first to be discovered [11], and *Bacteroides fragilis* (CcrA) [12]. Subclass B2 contains the very similar *Aeromonas* enzymes, CphA [13] and ImiS [14].

Subclass B3 consists of the L1 [15], FEZ-1 [16], GOB-type enzymes [17,18], Thin-B [19], CAU-1 [20], Mbl1b [21], BJP-1 [22] and CAR-1 [23]. However, only the first three are clinically relevant. L1 exhibits the

Abbreviations
ICP, inductively coupled plasma; IPTG, isopropyl β-D-1-thiogalactopyranoside; LB, Luria–Bertani; MBL, metallo-β-lactamase; TB, terrific broth.

broadest substrate range of the MBLs and is uniquely tetrameric [9,24,25]. FEZ-1 shares 29.7% sequence identity with L1, but has a more limited substrate profile, with a strong preference for cephalosporins [16,26]. GOB-type enzymes include 18 variants, including GOB-1, the first isolated GOB enzyme [17]. GOB-1 is from *Elizabethkingia meningoseptica* (formerly *Chryseobacterium meningosepticum*), the pathogen responsible for neonatal meningitis, and also found to attack immunocompromised patients. It shares sequence identities of 28% with L1 and 43% with FEZ-1 (computation performed at the SIB using the BLAST network service). The GOB-18 variant studied by Moran-Barrio *et al*. [18] differs from GOB-1 by just three residues, Phe94, Ala137 and Asp282, far from the active site.

The three subclasses of MBLs also differ in their zinc dependency [7]. Subclass B1 enzymes can be active with one or two zinc ions in their active sites, whereas those of subclass B3 contain two zinc ions [27,28]. In contrast, subclass B2 enzymes are active with one zinc ion and are inhibited by the binding of a second zinc [29]. The crystal structures of the MBLs highlight two sites of zinc co-ordination. The first zinc site in classes B1 and B3 (HHH) is composed of residues His116, His118 and His196. The sole exceptions to this are the GOB enzymes, which have a glutamine at position 116. In subclass B2, position 116 is occupied by an asparagine residue [7] and this was previously thought to be one of the residues to which the inhibitory zinc binds. However, the recent structure of the subclass B2 CphA showed that the second inhibitory zinc ion was just bound to the two remaining histidines, His196 and His118 [30]. The second zinc site of subclass B1 is identical to the first site of subclass B2 and consists of Asp120, Cys221 and His 263 (DCH), whereas in subclass B3, Cys221 is replaced by His121 (DHH) as a zinc ligand [7,15,26].

Even though the GOB enzymes appear to have only one intact zinc-binding site, they were placed in subclass B3 on the basis of their amino acid sequences [17]. However, unlike L1 [24] they are monomeric and unlike FEZ-1 [18] show no preference for cephalosporins [17]. The crystal structures of both L1 and FEZ-1 have been published [15,26], whereas the structure of a GOB-type enzyme has yet to be solved. Recent work by Moran-Barrio *et al*. [18] suggests that the active form of the enzyme contains only one zinc ion, located in the DHH site. This is in contrast to all known B1 and B3 MBLs, with the possible exception of the mono-Co^{++} form of BcII [31]. In the work described here, we produced the GOB-1 MBL in *Escherichia coli* from a T7-based expression vector. The results presented herein provide evidence for the presence of two zinc ions in the enzyme as purified. Therefore, in contrast to the GOB-18 variant [18], denaturing and refolding in the presence of zinc was not required. Although the outcome of the kinetic study, performed in the presence and absence of additional zinc, varied with the replacing residue, each Gln116 mutant showed a significant decrease in activity when compared with the wild-type enzyme.

Results

Construction of expression vector and preliminary expression experiments

The pGB1 expression vector was constructed to include the enzyme's own signal peptide and stop codon. The preliminary expression trials showed that the best yield was obtained in terrific broth (TB) medium in the absence of isopropyl β-D-1-thiogalactopyranoside (IPTG) with incubation at 28 °C for 24 h and showed no noticeable expression of the unprocessed precursor species. Under these conditions, GOB-1 represented only a low percentage of cell protein, but significantly more than with the pBS3 plasmid, previously described in Bellais *et al*. [17]. Unfortunately, with the crude extracts derived from the expression trials, activation by the substrate was observed, which made quantification difficult. This prevented an accurate determination of the quantity of GOB-1 present in the crude extract, but an estimate using the highest rate suggested that ~40 mg of GOB-1 was produced per litre of culture.

Purification of wild-type GOB-1

The reported purifications of several MBLs utilize an S-Sepharose column as the first purification step. When applied to GOB-1, this step yielded an enzyme with few contaminants. The second step was an UNO S12 column and allowed the removal of some impurity, but was not sufficient to reach homogeneity. A further purification step on a molecular sieve removed the two remaining contaminants of lower molecular masses. After the three purification steps, 7.6 mg of GOB-1 were produced, showing no contaminants by SDS/PAGE. The use of the molecular sieve column also confirmed a 30 kDa molecular mass and thus a monomeric structure, as shown by Bellais *et al*. [17].

MS and N-terminal sequencing of wild-type GOB-1

The ESI-TOF MS spectra of the denatured protein (data not shown) showed two peaks, indicating the

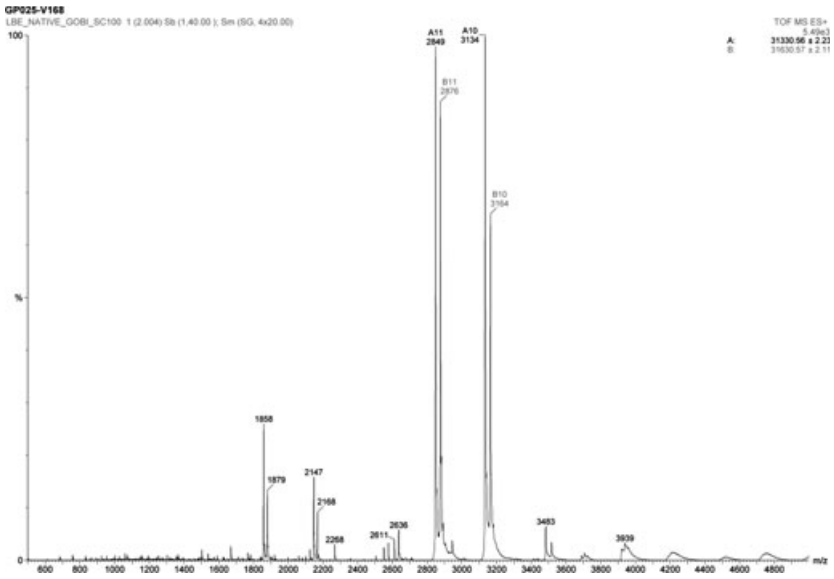

Fig. 1. ESI-TOF MS of wild-type GOB-1 showing the presence of two protein peaks separated by ~300 Da.

presence of two proteins separated by 299 Da. The native ESI-TOF MS spectra (Fig. 1) also showed two peaks separated by 300 Da. This showed the presence of two proteins that could not be separated during purification and by SDS/PAGE and that contained the same amount of zinc. This implied that both proteins were GOB-1, although one was modified in some way, probably by incorrect cleavage of the signal peptide to create β-lactamase ragged ends.

The mass difference between the native and denatured spectra corresponds to the mass of zinc in the enzyme (Table 1). The result suggests that the native protein contains two zinc ions per wild-type molecule. The other members of subclass B3, both L1 and FEZ-1, also contain two zinc ions in their active sites [9,10].

To verify the hypothesis that GOB-1 has ragged ends (not a unique phenomenon with respect to MBLs [32]), the N-terminus of the enzyme was sequenced. The presence of two N-terminal sequences QVVKE and LNAQV confirmed that the signal peptide was cleaved at two positions.

Table 1. Masses of the wild-type and mutant enzymes measured by ESI-TOF MS and calculated from their amino acid sequences. The calculated difference between measured masses of the denatured and native wild-type and mutant enzymes corresponds to the mass of zinc present in the enzyme.

GOB-1 enzyme	Calculated	Denatured	Native	Difference
Wild-type	31196.5	31195.5	31321	125.5
Q116A	31139.0	31138.5	31202	63.5
Q116N	31182.0	31183.0	31243	60.0
Q116H	31205.5	31206.0	31331	125.0

In addition, a sample was digested using trypsin and the molecular mass of the resulting peptides was measured by MALDI-TOF MS (Fig. 2). A theoretical digestion of GOB-1 was performed using Peptide Mass on the expasy.org website. The sequence coverage given by the peptides produced by the tryptic digestion of GOB-1 is shown in Fig. S1. All the peaks detected by MALDI-TOF MS could be identified as peptides produced by the tryptic digestion, with three exceptions. The peak at 1598 (Fig. 2) is not a theoretical product of digestion. It does, however, correspond to the mass of the N-terminal peptide (1299 kDa) plus 298 Da, a value that in turn corresponds to the mass of the last three amino acids of the signal peptide, LNA. Another of the unidentified peptides, of mass 1282, is the mass of the N-terminal peptide less 17 Da, suggesting that the N-terminal glutamine residue has undergone cyclization into pyro-glutamate with the loss of NH_3. The third peak at 1453 kDa could not be explained and does not correspond to digestion of the enzyme or unprocessed precursor species.

Mutation of the Gln116 residue

At position 116, GOB-1 has a glutamine rather than a histidine residue like other members of subclass B3 (or indeed subclass B1). To investigate the effect of this residue it was mutated to histidine, asparagine (the amino acid at position 116 in subclass B2) and, as a control, alanine, giving the Q116H, Q116N and Q116A mutants, respectively.

The best purification method found for the mutant enzymes was to use the S-Sepharose column, followed by a 5 mL Econo-Pac CHT-II cartridge. The remaining

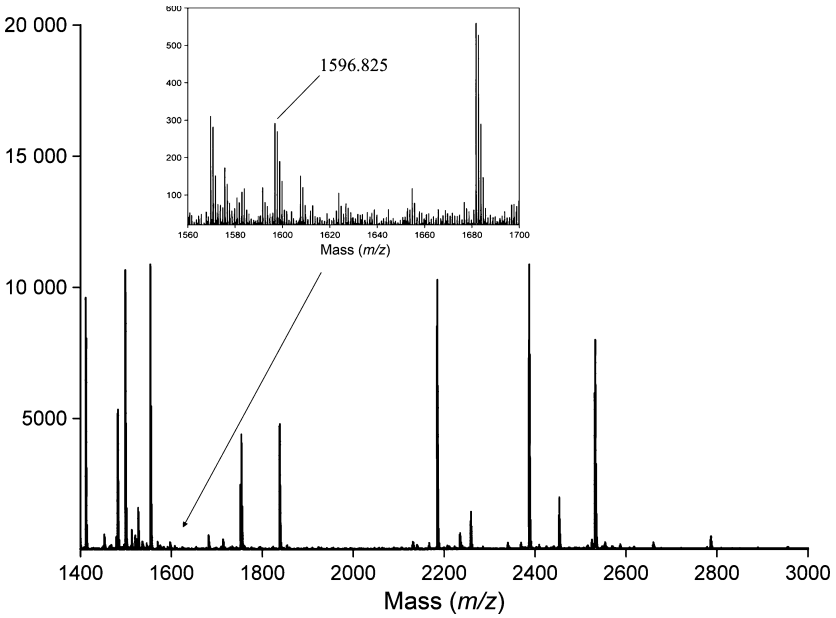

Fig. 2. Peptide mass fingerprint of GOB-1 digested by trypsin for 4 h (inset: N-terminus modified peptide with mass accuracy of 10 p.p.m.).

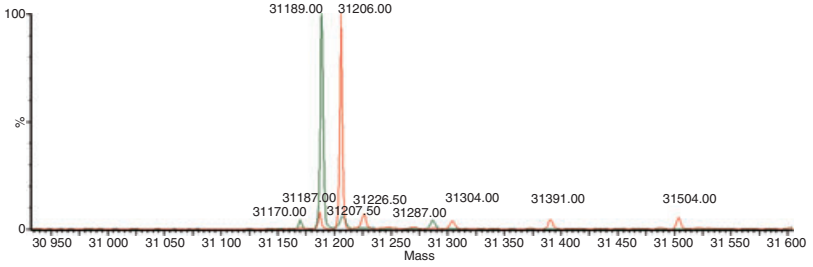

Fig. 3. Superimposed ESI-TOF MS of the two active peaks produced during the final step of purification of the Q116H mutant.

impurities were removed in a third purification step on an S-Source column. This last step produced two elution peaks for each enzyme. In each case, the mass difference between the two elution peaks was found to be 18 Da by ESI-TOF MS (Fig. 3) and the highest peak corresponded to the theoretically calculated mass. As a consequence, the N-terminal residue of the mutants has undergone partial cyclization. The protein of highest molecular mass (Table 1) was used in all experiments.

MS of GOB-1 mutants

Native ESI-TOF MS spectra of the mutants were obtained. Although Fig. 4 reveals the presence of many salt peaks, the spectra suggest that both Q116N and Q116A contain one zinc ion per molecule. This was confirmed by the inductively coupled plasma (ICP)/MS results (see below). Therefore, the mutation of the glutamine residue at position 116 results in the loss of zinc from the corresponding site of the enzyme under MS conditions. Q116H, like the wild-type, contains two zinc ions (Tables 1, 2).

Determination of the zinc and iron contents using ICP/MS

In contrast to the wild-type and Q116H enzymes, ICP/MS failed to highlight the binding of two zinc ions by the Q116A and Q116N enzymes (Table 2). Moreover, the ICP/MS discarded the presence of bound iron in all the enzymes.

Kinetic study

Before the kinetic characterization of GOB-1, the optimum concentration of $ZnCl_2$ in the buffer was determined. At the three concentrations of imipenem tested, the addition of Zn^{2+} in the buffer did not significantly modify the activity. However, 50 μM $ZnCl_2$ gave a slightly higher rate of hydrolysis. Consequently, 50 μM $ZnCl_2$ was thereafter added to the buffer.

The steady-state kinetic parameters of the wild-type and mutant GOB-1 enzymes were measured with the β-lactam substrates benzylpenicillin, cefoxitin, cephalothin, imipenem, meropenem and nitrocefin, both in the

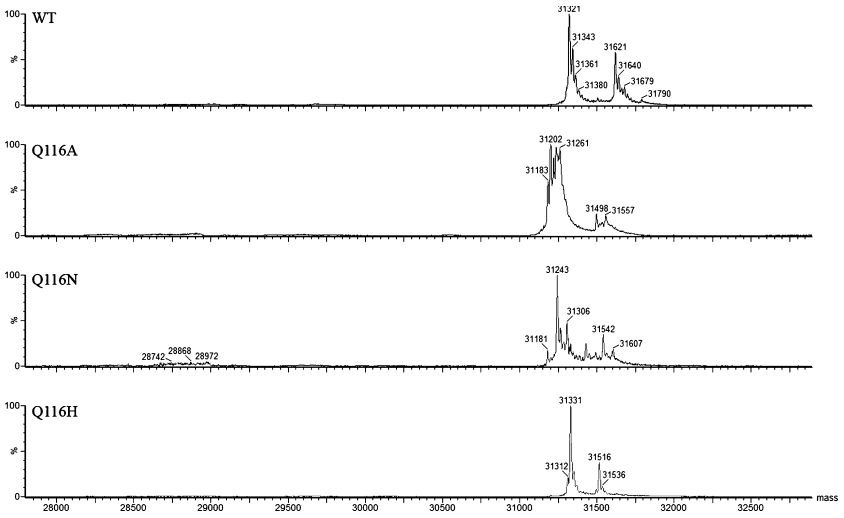

Fig. 4. Native ESI-TOF MS of the wild-type and mutant GOB-1.

presence and the absence of added zinc. The results are shown in Table 3. The wild-type enzyme hydrolysed all the substrates very efficiently, almost independently of the zinc concentration in the buffer, showing no strong preference for any type of β-lactam. Our results support those previously reported for GOB-1 [17], with the enzyme showing the highest rate of substrate turnover with penicillin (k_{cat} 630 s^{-1}) and the highest k_{cat}/K_M value with meropenem (8.0 $\mu M^{-1}.s^{-1}$).

The mutations of Gln116 significantly affected the catalytic ability of the enzyme, as would be expected for a zinc-binding residue. In the absence of added zinc, the activity was decreased 60–600-fold when the residue was mutated to the nonchelating alanine (Q116A). However, the resulting enzyme was not completely inactive and although the k_{cat} values were dramatically decreased, the K_m values were very similar. Activity was not restored by the addition of 50 μM zinc. Indeed, although k_{cat} values slightly increased (e.g. 4.6-fold for imipenem), the k_{cat}/K_m values slightly decreased due to the large increase in K_M values (34-fold for imipenem).

The effects of the Q116N mutation were slightly different. The results in Table 2 show an important loss of activity in the absence of zinc (160–1500 times), mainly due to a decrease in k_{cat} values. The K_M values remained quite similar (meropenem, cefoxitin), slightly (imipenem, benzylpenicillin) or significantly increased (nitrocefin, cephalothin). In contrast to the Q116A mutant, the activity of the Q116N mutant increased when 50 μM zinc was present in the buffer (Q116N is then only 1.3–110-fold less active than the wild-type). K_M values were similar to that of the wild-type (with the exception of nitrocefin). Initial hydrolysis rates of 100 μM nitrocefin were measured in the presence of increasing zinc concentrations (0, 1, 2.5, 5, 10, 25, 50, 100, 250, 500 and 1000 μM). This experiment showed that the maximal rate is obtained at a 50 μM zinc concentration and is constant up to the highest tested concentration. The apparent dissociation constant for the second zinc ion (K_{D2}) determined from this graph was 2.5 ± 0.3 μM (Fig. S2).

The effects of the Q116H mutation were less drastic. The activity decrease in comparison with the wild-type enzyme was only 2.1–74-fold. The k_{cat} values decreased only 1.9- (for benzylpenicillin) to 50-fold (for imipenem). The K_M values significantly increased for all the substrates but meropenem and cefoxitin. Q116H showed similar k_{cat} and K_M values in the presence of 50 μM zinc.

Table 2. Summary of zinc binding for wild-type and mutants GOB-1. Standard deviation values were below 10%.

	Zn^{2+} content in a buffer containing less than 0.4 μM of free zinc	
Protein	MS	ICP/MS
Wild-type	2	2.0
Q116A	1	0.8
Q116N	1	0.9
Q116H	2	2.0

Apo-GOB-1 and the remetallated form

The GOB-1 apoprotein was devoid of β-lactamase activity that could be recovered by the addition of Zn(II). Remetallated GOB-1 bound 2 equivalents of zinc, as shown by ICP/MS and MS (Fig. S3). However, its activity was only 60% of that of the enzyme as isolated. The addition of zinc (50 μM, 100 μM or 1 mM) to the reaction medium did not significantly modify this activity.

Table 3. The steady-state kinetic parameters for the GOB-1 wild-type and mutants Q116A, Q116N and Q116H, both in the presence and in the absence of added 50 μM $ZnCl_2$.

	50 μM zinc			No added zinc		
	K_M (μM)	k_{cat} (s^{-1})	k_{cat}/K_M ($\mu M^{-1} \cdot s^{-1}$)	K_M (μM)	k_{cat} (s^{-1})	k_{cat}/K_M ($\mu M^{-1} \cdot s^{-1}$)
Wild-type						
Imipenem	13 ± 1	85 ± 2	6.5	18 ± 0.6	77 ± 2	4.2
Meropenem	22 ± 1	170 ± 3	8.0	29 ± 1	100 ± 7	3.5
Benzylpenicillin	190 ± 10	630 ± 10	3.4	130 ± 6	540 ± 7	4.2
Nitrocefin	16 ± 3	14 ± 0.5	0.87	7.1 ± 0.2	20 ± 2	2.8
Cephalothin	7.9 ± 0.5	32 ± 0.4	4.0	3.8 ± 0.1	24 ± 0.7	6.5
Cefoxitin	8.9 ± 1	9.6 ± 0.4	1.1	1.4 ± 0.04	3.5 ± 0.3	2.6
Q116A						
Imipenem	720 ± 100	2.3 ± 0.2	0.0032	21 ± 0.9	0.50 ± 0.005	0.024
Meropenem	130 ± 20	1.1 ± 0.05	0.0088	34 ± 3	0.62 ± 0.02	0.018
Benzylpenicillin	410 ± 40	4.6 ± 0.1	0.011	96 ± 10	1.9 ± 0.08	0.020
Nitrocefin	30 ± 4	0.12 ± 0.002	0.0038	13 ± 1	0.080 ± 0.003	0.0062
Cephalothin	42 ± 4	0.61 ± 0.01	0.015	15 ± 0.7	0.16 ± 0.002	0.011
Cefoxitin	78 ± 10	0.21 ± 0.009	0.0027	7.2 ± 0.09	0.31 ± 0.01	0.043
Q116N						
Imipenem	42 ± 4	3.8 ± 0.1	0.025	69 ± 6	0.95 ± 0.03	0.014
Meropenem	20 ± 2	1.5 ± 0.03	0.074	31 ± 3	0.44 ± 0.01	0.014
Benzylpenicillin	140 ± 10	22 ± 0.5	0.16	200 ± 10	4.9 ± 0.1	0.025
Nitrocefin	360 ± 60	11 ± 0.9	0.031	210 ± 40	0.86 ± 0.06	0.0041
Cephalothin	4.7 ± 0.1	1.2 ± 0.05	0.25	37 ± 4	0.16 ± 0.004	0.0044
Cefoxitin	10 ± 0.3	0.16 ± 0.01	0.016	2.3 ± 0.1	0.026 ± 0.003	0.011
Q116H						
Imipenem	170 ± 20	21 ± 0.7	0.13	150 ± 10	17 ± 0.5	0.12
Meropenem	25 ± 3	2.3 ± 0.07	0.089	17 ± 2	2.0 ± 0.05	0.11
Benzylpenicillin	790 ± 40	300 ± 6	0.38	850 ± 60	280 ± 7	0.33
Nitrocefin	43 ± 6	3.5 ± 0.1	0.080	43 ± 4	1.6 ± 0.05	0.038
Cephalothin	64 ± 4	9.9 ± 0.2	0.15	57 ± 6	8.0 ± 0.3	0.14
Cefoxitin	1.8 ± 0.1	0.27 ± 0.03	0.15	2.5 ± 0.06	0.37 ± 0.03	0.15

Inactivation by metal chelator

EDTA inactivated GOB-1 and its mutants in a time-dependent manner. The k_i was independent of chelator concentration for the wild-type and mutant enzymes (Fig. S4). This suggests that EDTA acts by scavenging the free metal, with the k_i value representing the rate of zinc dissociation from the enzyme. The k_i value of wild-type GOB-1 was measured in the concentration range 0.5–50 μM, similar to those used to inactivate the other B3 enzymes L1 [24] and FEZ-1 [10] (up to 200 μM and 0.5–10 μM, respectively), indicating k_i values of ~0.0053 s^{-1}. This result is not very different from that obtained with FEZ-1 (0.025 s^{-1}) [10]. By comparison, incubation of IMP-1 (subclass B1) with 10 mM EDTA for 1 h only inactivated the enzyme by 10% [33]. The mutants behaved in a similar manner and the following k_i values were obtained: Q116A, 0.0044 s^{-1}; Q116H, 0.0068 s^{-1} and Q116N 0.011 s^{-1}. In the cases of the di-zinc species (i.e. the wild-type and Q116H), these rather similar apparent k_i values might correspond to the loss of the most tightly bound Zn^{++}.

Discussion

The MBL GOB-1 is a very efficient enzyme that hydrolyses the six tested β-lactams with k_{cat}/K_M values above 10^6 $M^{-1} \cdot s^{-1}$. All the k_{cat}/K_M values reported here are slightly higher (between 1.5- and 10-fold) than those previously published by Bellais *et al.* [17], probably because of the higher protein purity. The kinetic parameters determined here for the GOB-1 enzyme are also similar to those previously determined for the GOB-18 variant [18].

The mutants of GOB-1 generated by site-directed mutagenesis of Gln116 exhibit a loss of activity that cannot be corrected by the addition of zinc. The Q116H mutant and the wild-type enzyme both contain two zinc ions in the active site and therefore show little difference upon the addition of further zinc. However, the mutant exhibited significantly less activity than the

wild-type GOB-1 (k_{cat} shows a two- to 50-fold decrease, dependent upon which substrate is examined) and increased K_m values, suggesting than the steric effect of the larger, less flexible histidine residue hinders the positioning of the substrates in the active site. Another possibility would be the creation of a modified zinc position in the recreated HHH site leading to a decreased efficiency. However, as all other B1 and B3 enzymes include a histidine at position 116, this will remain speculation until the structure of the GOB-1 active site is directly determined.

In contrast to the Q116H mutant, the presence of an alanine or an asparagine residue at position 116 decreased the ability of the latter mutants to chelate a zinc ion in the AHH or NHH site. Indeed, in the absence of added zinc ([Zn] < 0.5 μM), these mutants were under a mono-zinc form, whereas the wild-type GOB-1 is already in a di-zinc form. The K_m values determined in these conditions for the Q116A mutant are very similar to those corresponding to the wild-type enzyme. This suggests that the Q116A mutation, which affects the metal content, does not affect the binding of the substrates. A similar behaviour is observed for the carbapenemase activity of the Q116N mutant.

This decreased ability to chelate a second zinc is also reflected by the K_{D2} value determined for the Q116N mutant. These results prove that Q116 plays a role in the binding of the zinc ion in the QHH site. The k_{cat} and k_{cat}/K_m values of the Q116A and Q116N mutants were strongly decreased (k_{cat} shows an 11–284-fold decrease for Q116A and a 23–227-fold decrease for Q116N compared with that of the wild-type) and cannot be restored by the addition of zinc. Nevertheless, the activity of the Q116N mutant increased with increasing zinc concentration in the buffer. This contrasts with the subclass B2 enzymes, which also have an asparagine residue at this position [7], as they are inhibited upon binding of a second zinc ion. However, it was demonstrated by Bebrone *et al.* [30] that this inhibition results from immobilization of the catalytically important His118 and His196 residues.

Our results differ from those obtained for the GOB-18 variant, which is supposed to be fully active with a single zinc ion in the DHH zinc-binding site [18]. GOB-1 and GOB-18 enzymes only differ by three point mutations apparently far from the active site (Leu94Phe, Ala137Val and Asp282Asn), which makes the difference in behaviour between these enzymes difficult to explain. GOB-18 was overproduced as a fusion to GST in the cytoplasm of *E. coli* and contained significant amounts of zinc and iron (0.45–0.75 iron/GOB-18 and 0.01–0.20 zinc/GOB-18). Only the mono-zinc form of GOB-18 could be obtained by remetallization of the apoprotein. Its activity largely exceeded that of the GOB-18 enzyme as isolated and the addition of zinc did not modify the kinetic parameters [18]. Further work by the same authors showed the periplasmic enzyme to contain only zinc ions, but the number remained unmeasured [18,34]. In contrast, the protocol of production and purification described here, which uses the enzyme's own signal peptide, produces GOB-1 as a fully active di-zinc enzyme. We have also shown that it is possible to reconstitute a binuclear GOB-1 from the metal-depleted enzyme by using a similar procedure to that previously described [18]. Furthermore, the Q116A and Q116N mutants that had lost the zinc in the QHH site showed a significantly decreased activity compared with that of the wild-type enzyme; the difference in both k_{cat} and the zinc content can only be accounted for by a single amino acid change if this is a zinc-binding residue.

GOB-1 is not a hybrid between subclasses B2 and B3, as previously suggested (Garau *et al.* [35]), but rather a new subclass B3 enzyme using a slightly smaller, more flexible, chelating residue. Surprisingly, this glutamine residue does not seem to be detrimental to the activity of the GOB enzymes when compared with the enzymes with a conventional HHH site.

Materials and methods

Chemicals

Buffers and BSA were purchased from BDH Chemicals (Poole, UK) or Sigma-Aldrich (Steinheim, Germany); IPTG from Eurogentech (Liège, Belgium) and kanamycin, dimethylsulfoxide and $ZnCl_2$ from Merck (Darmstadt, Germany). Meropenem ($\Delta\varepsilon_{300}$ = −6500 $M^{-1}\cdot cm^{-1}$) was a gift from ICI Pharmaceuticals (Macclesfield, UK). Imipenem ($\Delta\varepsilon_{300}$ = −9000 $M^{-1}\cdot cm^{-1}$) was a gift from Merck Sharpe and Dohme Research Laboratories (Rahway, NJ, USA). Benzylpenicillin ($\Delta\varepsilon_{235}$ = −775 $M^{-1}\cdot cm^{-1}$) was a gift from Rhône-Poulenc (Paris, France). Chloramphenicol, cefoxitin ($\Delta\varepsilon_{260}$ = −6600 $M^{-1}\cdot cm^{-1}$), cephalothin ($\Delta\varepsilon_{273}$ = −6300 $M^{-1}\cdot cm^{-1}$) and EDTA were purchased from Sigma (St Louis, MO, USA) and nitrocefin ($\Delta\varepsilon_{482}$ = 15 000 $M^{-1}\cdot cm^{-1}$) from Unipath Oxoid (Basingstoke, UK). Sequencing grade modified trypsin was obtained from Promega (Madison, WI, USA) and α-cyano-4-hydroxycinnamic acid was from Aldrich (Taufkirchen, Germany). The peptide standard mixture was purchased from Applied Biosystems (Foster City, CA, USA).

Bacterial strains and vectors

The plasmid pBS3 has been described previously. *Escherichia coli* DH5α was used as the host for recombinant plas-

mids during the construction of the expression vectors. *Escherichia coli* BL21-DE3 and *E. coli* BL21-DE3 (pLysS) (Novagen, Madison, WI, USA) were both tested as the hosts for the expression plasmids. The expression vector pET28a (Novagen) was used for the construction of the T7-based expression factor.

Construction of the expression vector and preliminary expression experiments

*Bam*H1 and *Xho*1 restriction sites were introduced at either end of the $bla_{GOB\text{-}1}$ gene by PCR using the oligonucleotide primers (5′-GGGGGGGGATCCATGAGAAATTTTGCTACACTGTTTTTCATG-3′) and (5′-CCCCCCCTCGAGTTATTTATCTTGGGAATCTTTTTTTATTTTGTC-3′), where the restriction sites generated are underlined. The PCR conditions were: incubation at 95 °C for 5 min; 30 cycles of amplification that involved denaturation for 1 min at 95 °C, annealing for 1 min at 58 °C and extension for 1 min at 68 °C; and 5 min at 68 °C after the cycling. *Pfu* and *taq* polymerase (Promega) were used for the PCR. The PCR products were cloned into the pET28a vector to obtain the recombinant plasmid pGB1, which was then transformed into *E. coli* DH5α. The gene was sequenced to verify that no unwanted mutations had taken place during the PCR.

The pGB1 vector was transformed into *E. coli* BL21-DE3 and BL21-DE3 (pLysS). Preliminary expression trials involved single colonies of *E. coli* BL21-DE3 and BL21-DE3 (pLysS) containing pGB1 used to inoculate 100 mL Luria–Bertani (LB), containing 50 $\mu g \cdot mL^{-1}$ kanamycin. The cultures were incubated overnight at 37 °C with orbital shaking at 250 r.p.m. before 2 mL samples were removed and added to 100 mL medium. Three types of medium, 2XYT (16 $g \cdot L^{-1}$ tryptone, 10 $g \cdot L^{-1}$ yeast extract, 5 $g \cdot L^{-1}$ sodium chloride), TB and LB, supplemented with 50 $\mu g \cdot mL^{-1}$ kanamycin were tested. After selection of the best medium, additional conditions were studied: two temperatures (28 and 37 °C), when the culture reached an absorbance of 0.6 at 600 nm and three different IPTG concentrations (0, 0.1 and 1 mM). Aliquots (2 mL) of the various cultures were sampled after 2, 4, 6, 24, 33 and 48 h. After centrifugation for 1 min at 15 000 ***g***, the bacterial pellet was resuspended in 500 μL buffer (Hepes; 20 mM at pH 6.5 containing 50 μM $ZnCl_2$). Cells were lysed by sonication on ice, which involved 5×15 s pulses with 30 s delays. The cell debris was removed by centrifugation at 15 500 ***g*** for 10 min at 4 °C. A 15 μL sample from each aliquot was analysed by SDS/PAGE.

The enzyme activity in each sample was determined by following the hydrolysis of 100 μM imipenem at 300 nm in 20 mM Hepes at pH 6.5 containing 50 μM $ZnCl_2$ using a Uvikon XL spectrophotometer and 10 mm path length cells.

Mutagenesis

The Quick Change site-directed mutagenesis kit (Stratagene, La Jolla, CA, USA) was used to perform the mutagenesis on the pGB1 plasmid. The primers used for this experiment were as follows:

For the Q116A mutant forward and reverse:

(5′-GATCTTGCTGCTTACTGCGGCTCACTACGACCATACAGG-3′)

(5′-GCACCTGTATGGTCGTAGTGAGCCGCAGTAAGCAGC-3′)

For the Q116N mutant forward and reverse:

(5′-GATCTTGCTGCTTACTAACGCTCACTACGACCATACAGG-3′)

(5′-GCACCTGTATGGTCGTAGTGAGCGTTAGTAAGCAGC-3′)

For the Q116H mutant forward and reverse:

(5′-GATCTTGCTGCTTACTCATGCTCACTACGACCATACAGG-3′)

(5′-GCACCTGTATGGTCGTAGTGAGCATGAGTAAGCAGC-3′)

Production and purification of the zinc β-lactamase

LB medium (100 mL) containing 50 $\mu g \cdot mL^{-1}$ kanamycin was inoculated with a colony of *E. coli* BL21-DE3 carrying the pGB1 plasmid and incubated overnight at 37 °C with orbital shaking at 250 r.p.m. Twenty millilitres of preculture were added to 2 L TB medium and incubated at 28 °C for 24 h under orbital shaking. Cells were harvested by centrifugation at 14 500 ***g*** for 20 min at 4 °C. The pellet was resuspended in 200 mL buffer A (20 mM sodium cacodylate, pH 6.5) before the cells were disrupted (Basic Z model; Constant Systems Ltd, Warwick, UK). Cell debris was removed by centrifugation at 14 300 ***g*** for 40 min at 4 °C and the supernatant dialysed overnight against buffer A at 4 °C. The crude extract was then loaded on to an S-Sepharose FF column (2.6×34 cm; Pharmacia, Uppsala, Sweden) equilibrated in buffer A. The column was washed with buffer A before a salt gradient of 0–0.5 M NaCl in five column volumes was used to elute the GOB-1 protein. The active fractions were pooled and dialysed overnight against buffer A to remove the salt. The sample was loaded on to an UNO S-12 column equilibrated with buffer A and eluted with a 0–0.5 M NaCl gradient in five column volumes. The fractions that showed β-lactamase activity were then loaded on to a Sephacryl-100 molecular sieve column (1.5×56 cm) previously equilibrated in buffer B (buffer A with 0.25 M NaCl). For molecular mass determination on this column, the following proteins were used for calibration; BSA 66.2 kDa, ovalbumin 45 kDa, soybean trypsin inhibitor 21.5 kDa, lysozyme 14.4 kDa. Active fractions were pooled, dialysed against buffer A and concentrated to a final concentration of approximately 1 $mg \cdot mL^{-1}$, before being stored at −20 °C.

The mutant plasmids were transformed into *E. coli* BL21-DE3 and production was carried out as described above for the wild-type. Purification was performed as described for the wild-type with the following modifications. The second column used was a 5 mL ceramic hydroxyapatite Econo-Pac CHT-II cartridge (Bio-Rad, Hercules, CA, USA). The purification was carried out as suggested in the manufacturer's instructions). The third column, an S-Source column from Amersham Biosciences (Piscataway, NJ, USA), was used to separate the desired mutants from the variant of the enzyme with an N-terminal pyro-glutamate residue. The enzyme was loaded and the column was washed in 20 mM sodium cacodylate pH 6.5 before a salt gradient of 0–0.5 M NaCl in 10 column volumes was used to elute the GOB-1 mutant.

MS and the determination of the N-terminal sequence

Native or denatured intact enzyme

Enzyme samples were desalted using Microcon YM-10 (10 kDa) centrifugal filters (Millipore, Billerica, MA, USA) in 15 mM ammonium acetate (pH 7.5). Seven dilution/concentration steps were performed at 4 °C and 14 000 ***g***. This yielded a 100 μM stock enzyme solution in ammonium acetate pH 7.5. The experimental samples were then prepared by diluting the enzyme to a final concentration of 15 μM in 15 mM ammonium acetate pH 7.5 directly in a 96-well plate. ESI-MS analyses used a Q-TOF MS (Q-TOFmicro Micromass, Altrincham, UK) interfaced with a NanoMate™ chip-based nano-ESI source (Advion Biosciences, Ithaca, NY, USA). Samples were infused into the Q-TOF through the ESI chip (estimated flow rate 100 $nL \cdot min^{-1}$). Typically, a spraying voltage of 1.70 kV ± 0.1 kV, depending on the 'sprayability' of the sample, and a sample pressure of 0.25 psi were applied. The instrument was equipped with a standard Z-spray source block. Clusters of $Cs_{(n+1)}I_n$ (1 $mg \cdot mL^{-1}$ CsI in 100% methanol) were used for calibration. Calibration and sample acquisitions were performed in the positive ion mode in the range of *m/z* 500–5000. Operating conditions for the MS were: sample cone voltage 50, 80 and 200 V, source temperature 40 °C. Acquisition and scan times were 20 and 1 s, respectively. The pressure at the interface between the atmospheric source and the high vacuum region was fixed at 6.6 mbar (measured with the roughing pump Pirani gauge) by throttling the pumping line using an Edwards Speedivalve to provide collisional cooling.

Peptide mapping

After denaturation at 100 °C for 15 min, 10 μg of GOB-1 was digested with 0.5 μg trypsin in 50 mM NH_4HCO_3 (pH 8) for 4 h at 37 °C. The digestion was stopped by adding 0.1% trifluoroacetic acid. Digested protein (10 μL) was loaded on to a ZipTip C18 (Millipore). Elution was performed with a 10 μL matrix solution (α-cyano-4-hydroxycinnamic acid in 50% acetonitrile, 0.1% trifluoroacetic acid) on a MALDI plate and dried before the MALDI measurement.

MS analysis was performed using a 4800 MALDI TOF/TOF™ analyser (Applied Biosystems/MDS SCIEX) equipped with a 200 Hz Nd:YAG-Laser (λ = 355 nm, 3–7 ns pulse width). MS data were acquired in the positive ion reflectron mode with 470 ns delayed extraction, accumulating 500 laser shots using the 4000 Series EXPLORER™ remote access client software (version 3.5.1). External mass calibration was performed in the mass range *m/z* of 800–3500. The calibration mixture consisted of the following compounds: des-Arg^1-bradykinin [904.4681], angiotensin I [1296.6853], Glu^1-fibrinopeptide B [1570.6774], adrenocorticotropic hormone fragments 1–17 [2093.0867], adrenocorticotropic hormone fragments 18–39 [2465.1989], adrenocorticotropic hormone fragments 7–38 [3557.9294]. For MS/MS measurements, the acceleration voltage was 8 kV, the laser energy 4090 and 4000 laser shots were accumulated.

N-terminal sequence

The N-terminal sequence was determined using a gas-phase sequencer (Prosite 492 protein sequencer; Applied Biosystems).

Determination of the zinc and iron content using ICP/MS

Protein samples were dialysed against 20 mM sodium cacodylate, pH 6.5. Protein concentrations were then determined by standard colorimetric assays (BCA; Pierce, Rockford, IL, USA). Zinc and iron concentrations were measured by ICP MS at the Malvoz Institute (Province de Liège, Belgium). The metal/enzyme ratio was calculated from the differences in metal concentration between the enzyme sample and the dialysis buffer.

Determination of kinetic parameters

Hydrolysis of antibiotics by the wild-type and mutant GOB-1 was monitored by following the variation in absorbance using a Uvikon 860 spectrophotometer connected to a microcomputer via an RS232 serial interface or a Uvikon XL spectrophotometer. Reactions were performed in thermostatically controlled 10 and 2 mm path length cells at 30 °C and using 20 mM sodium cacodylate buffer pH 6.5, containing 20 $\mu g \cdot mL^{-1}$ BSA (and 50 μM $ZnCl_2$ when indicated). The steady-state kinetic parameters were determined under initial rate conditions using the Hanes linearization of the Henri–Michaelis–Menten equation. Low K_M values were determined as K_is using meropenem as the reporter

substrate. In these cases, the k_{cat} values were obtained from initial hydrolysis rates measured at saturating substrate concentrations. All data were analysed using Microsoft Excel and the KALEIDAGRAPH 3.5 programme [36].

Enzymatic measurement in the presence of increasing concentrations of zinc and the determination of K_{D2}

Activity was measured in the presence of increasing concentrations of zinc at 30 °C in 20 mM sodium cacodylate buffer pH 6.5, containing 20 $\mu g \cdot mL^{-1}$ BSA, as previously described. The binding of the second zinc ion resulted in an increase in activity and equation 1 was used:

$$RA = [(K_{D2} + \alpha[Zn])/([Zn] + K_{D2})] \quad (1)$$

where α represents the ratio of activity at saturating zinc concentration versus activity in the absence of added zinc (Act. [Zn](∞)/Act. [Zn](0)).

Experimental data were fitted to equation 1 by nonlinear regression analysis with the help of the SIGMA PLOT software.

Preparation of the GOB-1 apoenzyme and the remetallated form

The GOB-1 apoprotein was prepared by treating ~40 μM enzyme samples in 10 mM Tris/HCl, pH 7.0, with chelating agents in mild denaturing conditions, as previously described for GOB-18 [18]. The remetallated form was obtained by dialysing the apo-GOB-1 against 100 volumes of 10 mM Tris/HCl, pH 7.0, 50 mM NaCl, with 40 μM $ZnSO_4$.

Inactivation by chelating agents

The inactivation of wild-type and mutant GOB-1 by the chelating agent EDTA was followed using imipenem as a reporter substrate and measuring the initial rates of hydrolysis at varying EDTA concentrations (0.5–50 μM), in the same buffer as that used for the other kinetic experiments, without the addition of zinc. The dependence of k_i on the concentration of chelating agent was investigated.

Acknowledgements

The authors thank Alain Dubus (GIGA MS platform, Université de Liège) who performed ESI-TOF MS additional experiments after conditions were found for the wild-type enzyme. We also thank Nicole Otthiers (Université de Liège) who performed the N-terminal sequencing. This work was supported by the Belgian Federal Government (PAI P5/33), grants from the FNRS (Brussels, Belgium, FRFC grants n° 2 4508.01, 2.4.524.03 and Lot. Nat. 9.4538.03), the European Research Training Network (MEBEL contract HPTR-CT-2002-00264) and the targeted programme COBRA, financed by the European Commission (no. LSHM-CT-2003-503335).

References

1 Carfi A, Pares S, Duee E, Galleni M, Duez C, Frere JM & Dideberg O (1995) The 3-D structure of a zinc metallo-beta-lactamase from *Bacillus cereus* reveals a new-type of protein fold. *EMBO J* **14**, 4914–4921.
2 Frere JM (1995) Beta-lactamases and bacterial-resistance to antibiotics. *Mol Microbiol* **16**, 385–395.
3 Matagne A, Dubus A, Galleni M & Frere JM (1999) The beta-lactamase cycle: a tale of selective pressure and bacterial ingenuity. *Nat Prod Rep* **16**, 1–19.
4 Wang ZG, Fast W, Valentine AM & Benkovic SJ (1999) Metallo-beta-lactamase: structure and mechanism. *Curr Opin Chem Biol* **3**, 614–622.
5 Ambler RP (1980) The structure of beta-lactamases. *Philos Trans R Soc Lond B* **289**, 321–331.
6 Bush K, Jacoby GA & Medeiros AA (1995) A functional classification scheme for beta-lactamases and its correlation with molecular-structure. *Antimicrob Agents Chemother* **39**, 1211–1233.
7 Galleni M, Lamotte-Brasseur J, Rossolini GM, Spencer J, Dideberg O & Frere JM (2001) Standard numbering scheme for class B beta-lactamases. *Antimicrob Agents Chemother* **45**, 660–663.
8 Valladares MH, Kiefer M, Heinz U, Soto RP, Meyer-Klaucke W, Nolting HF, Zeppezauer M, Galleni M, Frere JM, Rossolini GM *et al.* (2000) Kinetic and spectroscopic characterization of native and metal-substituted beta-lactamase from *Aeromonas hydrophila* AE036 (FEBS 23250) [*FEBS Lett* 467 (2000) 221–225]. *FEBS Lett* **477**, 285–285.
9 Crowder MW, Walsh TR, Banovic L, Pettit M & Spencer J (1998) Overexpression, purification, and characterization of the cloned metallo-beta-lactamase L1 from *Stenotrophomonas maltophilia*. *Antimicrob Agents Chemother* **42**, 921–926.
10 Mercuri PS, Bouillenne F, Boschi L, Lamote-Brasseur J, Amicosante G, Devreese B, Van Beeumen J, Frere JM, Rossolini GM & Galleni M (2001) Biochemical characterization of the FEZ-1 metallo-beta-lactamase of *Legionella gormanii* ATCC 33297(T) produced in *Escherichia coli*. *Antimicrob Agents Chemother* **45**, 1254–1262.
11 Baldwin GS, Galdes A, Hill HAO, Waley SG & Abraham EP (1980) A spectroscopic study of metal-ion and ligand-binding to beta-lactamase II. *J Inorg Biochem* **13**, 189–204.

12 Bandoh K, Muto Y, Watanabe K, Katoh N & Ueno K (1991) Biochemical properties and purification of metallo-beta-lactamase from *Bacteroides fragilis*. *Antimicrob Agents Chemother* **35**, 371–372.
13 Massidda O, Rossolini GM & Satta G (1991) The *Aeromonas hydrophila* Cpha gene - molecular heterogeneity among class-B metallo-beta-lactamases. *J Bacteriol* **173**, 4611–4617.
14 Walsh TR, Gamblin S, Emery DC, MacGowan AP & Bennett PM (1996) Enzyme kinetics and biochemical analysis of ImiS, the metallo-beta-lactamase from *Aeromonas sobria* 163a. *J Antimicrob Chemother* **37**, 423–431.
15 Ullah JH, Walsh TR, Taylor IA, Emery DC, Verma CS, Gamblin SJ & Spencer J (1998) The crystal structure of the L1 metallo-beta-lactamase from *Stenotrophomonas maltophilia* at 1.7 angstrom resolution. *J Mol Biol* **284**, 125–136.
16 Boschi L, Mercuri PS, Riccio ML, Amicosante G, Galleni M, Frere JM & Rossolini GM (2000) The *Legionella* (*Fluoribacter*) *gormanii* metallo-beta-lactamase: a new member of the highly divergent lineage of molecular-subclass B3 beta-lactamases. *Antimicrob Agents Chemother* **44**, 1538–1543.
17 Bellais S, Aubert D, Naas T & Nordmann P (2000) Molecular and biochemical heterogeneity of class B carbapenem-hydrolyzing beta-lactamases in *Chryseobacterium meningosepticum*. *Antimicrob Agents Chemother* **44**, 1878–1886.
18 Moran-Barrio J, Gonzalez JM, Lisa MN, Costello AL, Dal Peraro M, Carloni P, Bennett B, Tierney DL, Limansky AS, Viale AM *et al.* (2007) The metallo-beta-lactamase GOB is a mono-Zn(II) enzyme with a novel active site. *J Biol Chem* **282**, 18286–18293.
19 Rossolini GM, Condemi MA, Pantanella F, Docquier JD, Amicosante G & Thaller MC (2001) Metallo-beta-lactamase producers in environmental microbiota: new molecular class B enzyme in *Janthinobacterium lividum*. *Antimicrob Agents Chemother* **45**, 837–844.
20 Docquier JD, Pantanella F, Giuliani F, Thaller MC, Amicosante G, Galleni M, Frere JM, Bush K & Rossolini GM (2002) CAU-1, a subclass B3 metallo-beta-lactamase of low substrate affinity encoded by an ortholog present in the *Caulobacter crescentus* chromosome. *Antimicrob Agents Chemother* **46**, 1823–1830.
21 Simm AM, Higgins CS, Pullan ST, Avison MB, Niumsup P, Erdozain O, Bennett PM & Walsh TR (2001) A novel metallo-beta-lactamase, Mb11b, produced by the environmental bacterium *Caulobacter crescentus*. *FEBS Lett* **509**, 350–354.
22 Stoczko M, Frere JM, Rossolini GM & Docquier JD (2006) Postgenomic scan of metallo-beta-lactamase homologues in rhizobacteria: identification and characterization of BJP-1, a subclass B3 ortholog from *Bradyrhizobium japonicum*. *Antimicrob Agents Chemother* **50**, 1973–1981.
23 Stoczko M, Frere JM, Rossolini GM & Docquier JD (2008) Functional diversity among metallo-beta-lactamases: characterization of the CAR-1 enzyme of *Erwinia carotovora*. *Antimicrob Agents Chemother* **52**, 2473–2479.
24 Bicknell R, Emanuel EL, Gagnon J & Waley SG (1985) The production and molecular properties of the zinc beta-lactamase of *Pseudomonas maltophilia* IID 1275. *Biochem J* **229**, 791–797.
25 Saino Y, Kobayashi F, Inoue M & Mitsuhashi S (1982) Purification and properties of inducible penicillin beta-lactamase isolated from *Pseudomonas maltophilia*. *Antimicrob Agents Chemother* **22**, 564–570.
26 Garcia-Saez I, Mercuri PS, Papamicael C, Kahn R, Frere JM, Galleni M, Rossolini GM & Dideberg O (2003) Three-dimensional structure of FEZ-1, a monomeric subclass B3 metallo-beta-lactamase from *Fluoribacter gormanii*, in native form and in complex with D-captopril. *J Mol Biol* **325**, 651–660.
27 Paul-Soto R, Bauer R, Frere JM, Galleni M, Meyer-Klaucke W, Nolting H, Rossolini GM, de Seny D, Hernandez-Valladares M, Zeppezauer M *et al.* (1999) Mono- and binuclear Zn2 + -beta-lactamase – role of the conserved cysteine in the catalytic mechanism. *J Biol Chem* **274**, 13242–13249.
28 Paul-Soto R, Hernandez-Valladares M, Galleni M, Bauer R, Zeppezauer M, Frere JM & Adolph HW (1998) Mono- and binuclear Zn-beta-lactamase from *Bacteroides fragilis*: catalytic and structural roles of the zinc ions. *FEBS Lett* **438**, 137–140.
29 Valladares MH, Felici A, Weber G, Adolph HW, Zeppezauer M, Rossolini GM, Amicosante G, Frere JM & Galleni M (1997) Zn(II) dependence of the *Aeromonas hydrophila* AE036 metallo-beta-lactamase activity and stability. *Biochemistry* **36**, 11534–11541.
30 Bebrone C, Delbruck H, Kupper MB, Schlomer P, Willmann C, Frere JM, Fischer R, Galleni M & Hoffmann KMV (2009) The structure of the dizinc subclass B2 metallo-beta-lactamase CphA reveals that the second inhibitory zinc ion binds in the histidine site. *Antimicrob Agents Chemother* **53**, 4464–4471.
31 Llarrull LI, Tioni MF & Vila AJ (2008) Metal content and localization during turnover in *B. cereus* metallo-beta-lactamase. *J Am Chem Soc* **130**, 15842–15851.
32 Payne DJ, Skett PW, Aplin RT, Robinson CV & Knowles DJC (1994) Beta-lactamase ragged ends detected by electrospray mass-spectrometry correlates poorly with multiple banding on isoelectric focusing. *Biol Mass Spectrom* **23**, 159–164.
33 Laraki N, Franceschini N, Rossolini GM, Santucci P, Meunier C, de Pauw E, Amicosante G, Frere JM & Galleni M (1999) Biochemical characterization of the *Pseudomonas aeruginosa* 101/1477 metallo-beta-lactamase IMP-1 produced by *Escherichia coli*. *Antimicrob Agents Chemother* **43**, 902–906.

34 Moran-Barrio J, Limansky AS & Viale AM (2009) Secretion of GOB metallo-beta-lactamase in *Escherichia coli* depends strictly on the cooperation between the cytoplasmic DNAK chaperone system and the sec machinery: completion of folding and Zn(II) ion acquisition occur in the bacterial periplasm. *Antimicrob Agents Chemother* **53**, 2908–2917.
35 Garau G, Bebrone C, Anne C, Galleni M, Frere JM & Dideberg O (2005) A metallo-beta-lactamase enzyme in action: crystal structures of the monozinc carbapenemase CphA and its complex with biapenem. *J Mol Biol* **345**, 785–795.
36 Cornish-Bowden A (2004) *Fundamentals of Enzyme Kinetics*, 3rd edn. Portland, London.

Supporting information

The following supplementary material is available:
Fig. S1. GOB-1 sequence, including the LNA from the signal peptide. Peptides from the tryptic digestion identified by MALDI-TOF MS are highlighted to show the sequence coverage. Peptides either have one or no sites of missed cleavage; no peptides with two or more missed cleavage sites were identified.
Fig. S2. Relative activity of the Q116N mutant measured in the presence of increasing concentrations of zinc.
Fig. S3. Native ESI-TOF MS of the remetallated GOB-1.
Fig. S4. Graph showing the effect of varying EDTA concentration on the k_i of the GOB-1 enzymes.

This supplementary material can be found in the online version of this article.

Please note: As a service to our authors and readers, this journal provides supporting information supplied by the authors. Such materials are peer-reviewed and may be re-organized for online delivery, but are not copy-edited or typeset. Technical support issues arising from supporting information (other than missing files) should be addressed to the authors.